

Therefore, for weak shock waves, Eq. (13) can give β values that approach the accurate values over a wide range of M_1 and θ . With Eq. (13), β is evaluated easily from the values of θ and M_1 .

References

- ¹Liepmann, H. W., and Roshko, A., *Elements of Gasdynamics*, Wiley, New York, 1957, pp. 84-93.
- ²Anderson, J. D., Jr., *Fundamentals of Aerodynamics*, McGraw-Hill, New York, 1984, pp. 347-359.
- ³Kuethe, A. M., and Chow, C. Y., *Foundations of Aerodynamics: Bases of Aerodynamic Design*, 4th ed., Wiley, New York, 1986, pp. 225-229.

Using Rankine Vortices to Model Flow Around a Body of Revolution

B. S. Taylor*

Portsmouth Polytechnic, Hampshire Terrace,
Portsmouth, England, United Kingdom
and

A. R. J. M. Lloyd†

Defense Research Agency, Haslar, Gosport,
PO12 2AG, England, United Kingdom

I. Introduction

IN Refs. 1 and 2, Lloyd described SUBSIM, a mathematical model to simulate deeply submerged maneuvers of a submarine. The model is based on a time-marching simulation of the changing flow around the maneuvering submarine and takes account of the vortices shed from the appendages and the separated flow on the hull. Similar techniques have been used to compute the maneuvering characteristics of missiles (see Ref. 3).

The flow around the submarine is described in terms of a distribution of shed vortices where the characteristics of the appendage vortices are computed using Glauert's⁴ lifting-line theory while the vorticity shed from the hull is modeled using a total of 22 vortices. The positions and strengths of these are computed from empirical data measured on a submarine-like body of revolution (rounded nose and pointed tail) on the Rotating Arm facility at the Admiralty Research Establishment, Haslar, England, UK. The experiments were described by Lloyd and Campbell⁵ and Lloyd.⁶ They involved the direct measurement of vorticity using a Freestone probe⁷ and the integration of vorticity contours to obtain circulation as a function of the body station, nondimensional turn rate, and drift velocity. Empirical equations fitted to the results are used to compute the strength and position of the hull vortices in SUBSIM.

Classical potential flow techniques are used to compute the velocities in planes transverse to the axis of the submarine. This allows the computation of the trajectories of the appendage vortices and also the calculation of the local incidence at various spanwise stations on each appendage. These local incidences are then used in the lifting-line calculations.

II. Rankine Vortex

In the early development of the mathematical model, classical inviscid vortices were used with the velocity field given by

$$q = q_\psi \hat{\psi} = \frac{\Gamma}{2\pi R} \hat{\psi}$$

where Γ is the circulation, (R, ψ, z) refer to a system of cylindrical polar coordinates with the vortex at $R = 0$, and $\hat{\psi}$ is a unit vector in the direction of increasing ψ .

The appropriate circulation of each vortex can be calculated, but the viscosity is zero everywhere except on the vortex filament itself where it is undefined. This is obviously not consistent with the experimental data. This approach also leads to the prediction of very large incidences when a vortex is close to an appendage.

For these reasons, it is more realistic to use the Rankine formulation

$$q = q_\psi \hat{\psi} = \frac{\Gamma}{2\pi R} [1 - \exp(-\alpha R^2)] \hat{\psi} \quad (1)$$

where α is a constant. It is evident that this is equivalent to an inviscid vortex for large R , and since $q = (\Gamma\alpha R)/2\pi$ for small R , the vortex behaves as if it has a solid core.

The core radius R_* is defined to be the radius at which maximum speed occurs, and so $dq_\psi/dR = 0$ at $R = R_*$. From Eq. (1), it follows that $2\alpha R_*^2 + 1 = \exp(\alpha R_*^2)$, which gives the solution $\alpha = 1.26/R_*^2$.

The separated flow from the hull is modeled by a string of Rankine vortices. The circulation and core radius of each vortex is calculated from the experiment data. However, if the vortices are too far apart, they will retain their individual identity and produce discrete sets of nominally circular contours. We need to devise a test to establish whether the vortices will merge to produce continuous vorticity contours, representative of those measured in the experiment.

III. Mathematical Condition for Merging

For two vortices of equal circulation and core radius at $(D, 0)$ and $(-D, 0)$, the magnitude of the vorticity $\zeta = \text{curl } \underline{q}$ at points on the x axis is given by

$$= \frac{1.26\Gamma}{\pi R_*^2} \left\{ \exp \left[-1.26 \frac{(D-x)^2}{R_*^2} \right] + \exp \left[-1.26 \frac{(D+x)^2}{R_*^2} \right] \right\}$$

relative to an origin midway between the vortices.

Putting $y = x/D$ and $s = R_*/D$, this becomes

$$\zeta' = \frac{\pi D^2 \zeta s^2}{1.26\Gamma} = \left\{ \exp \left[-1.26 \left(\frac{1-y}{s} \right)^2 \right] + \exp \left[-1.26 \left(\frac{1+y}{s} \right)^2 \right] \right\}$$

The nondimensional vorticity ζ' is plotted for various values of the nondimensional core radius in Fig. 1. It can be seen that for small values of the core radius the vorticity distribution indicates two distinct vortices. As the core radius increases, the vortices merge. Now,

$$\frac{d\zeta'}{dy} = \frac{2.52}{s^2} \left\{ (1-y) \exp \left[-1.26 \left(\frac{1-y}{s} \right)^2 \right] - (1+y) \exp \left[-1.26 \left(\frac{1+y}{s} \right)^2 \right] \right\}$$

The vorticity is a maximum (or minimum) when $d\zeta'/dy = 0$ and this occurs when

$$\frac{1-y}{1+y} = \exp \left[-5.04 \frac{y}{s^2} \right] \quad (2)$$

Received Dec. 17, 1990; revision received May 7, 1991; accepted for publication May 13, 1991. Copyright © 1991 by the American Institute of Aeronautics and Astronautics, Inc. All rights reserved.

*Principal Lecturer.

†Principal Scientific Officer, Maritime Division.

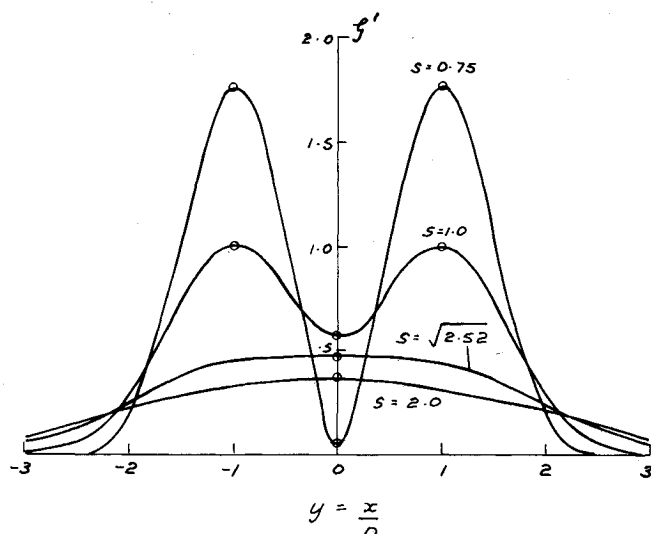


Fig. 1 Distribution of nondimensional vorticity along x axis. Vortices at $x = -D$ and $+D$ with various core radii. Vortices merge for $s > \sqrt{2.52}$.

To find the roots of Eq. (2), we draw graphs of

$$z = \frac{1-y}{1+y}$$

and

$$z = \exp \left[-5.04 \frac{y}{s^2} \right]$$

on the same axes as shown in Fig. 2.

There is always a point of intersection at $y = 0$, indicating a maximum or minimum at the origin. For small values of the nondimensional core radius s , there are two additional points of intersection that correspond approximately to the individual vortices.

The vortices merge if there is only one turning point, and this occurs if the gradient of

$$z = \frac{1-y}{1+y}$$

is less than the gradient of

$$z = \exp \left[-5.04 \frac{y}{s^2} \right]$$

at $y = 0$.

Hence, for merging we have

$$\frac{-(1+y) - (1-y)}{(1+y)^2} < -\frac{5.04}{s^2} \exp \left[-5.04 \frac{y}{s^2} \right]$$

when $y = 0$.

As a result, we have

$$-2 < -\frac{5.04}{s^2}$$

giving

$$s > \sqrt{2.52}$$

Hence, the condition for merging is approximately

$$R^* > 1.6D$$

or

$$R^* > 0.8d \quad (3)$$

where d is the separation between the vortices.

If the vortices are not equal, the situation is more involved and no longer results in a simple condition. The presence of other vortices enhances merging (i.e., the vortices need not be quite so close). Condition (3) provides a useful rule of thumb that has led to the decision to use 22 hull vortices in SUBSIM.

IV. Image System for a Circle

To describe the flow past a body in terms of Rankine vortices, we must also determine the appropriate image system.

We consider a vortex of circulation Γ at $(c, 0)$ outside the circle

$$x^2 + y^2 = a^2 \quad (a < c)$$

For an inviscid vortex, it is easily shown using Milne-Thomson's circle theorem that the image system consisting of a vortex of circulation $-\Gamma$ at the inverse point $[a^2/c, 0]$ together with a vortex of circulation Γ at the origin.

For a Rankine vortex, it is not possible to use the complex potential approach. Essentially the condition is that the circle is a streamline (i.e., the velocity on the circle is tangential to it). The vortex at the origin is not relevant in this respect. It is included to make the circulation around the circle zero.

The velocities v_1 and v_2 produced by the original vortex and the vortex at the inverse point produce a resultant velocity $v_1 + v_2$, which is tangential to the circle.

With a Rankine vortex, v_1 will be in the same direction but with smaller magnitude than with an inviscid vortex. Provided that the magnitude of v_2 is reduced in proportion, then $v_1 + v_2$ will still be in the same direction. Hence, for the circle to remain a streamline with a Rankine vortex, we require

$$1 - \exp \left[-1.26 \frac{R^2}{R_*^2} \right] = 1 - \exp \left[-1.26 \frac{R^2}{R_*^2} \right]$$

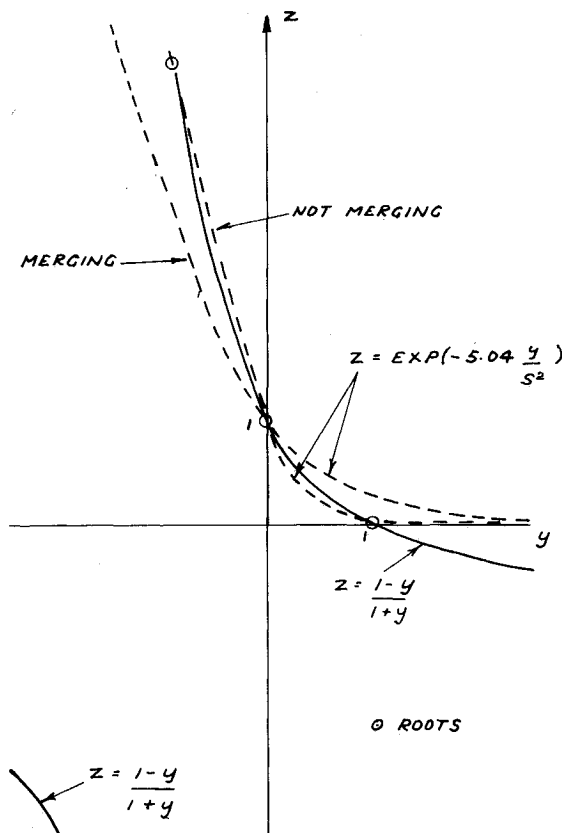


Fig. 2 Functions $z = (1-y)/(1+y)$ and $z = \exp [-5.04(y/s^2)]$.

where R , R_* refer to the original vortex and R' , R'_* to the image vortex at the inverse point.

As a result, we conclude that

$$\frac{R}{R_*} = \frac{R'}{R'_*}$$

or

$$R'_* = \frac{R'}{R} R_* \quad (4)$$

However, the equation of the circle can be written in the form

$$\frac{R'}{R} = \frac{a - (a^2/c)}{c - a} = \frac{a}{c}$$

since in Cartesian coordinates this becomes

$$\frac{(x - a^2/c)^2 + y^2}{(x - c)^2 + y^2} = \frac{a^2}{c^2}$$

which gives on simplification

$$x^2 + y^2 = a^2$$

It follows from Eq. (4) that the core radius of the image vortex at the inverse point is R'_* , where

$$R'_* = \frac{a}{c} R_*$$

Since the core radius of the vortex at the origin does not affect the condition of tangential velocity at the circle and since we will not be interested in points inside the circle, it is proposed to use an inviscid vortex at the origin.

V. Conclusions

This paper has described the techniques used in the SUBSIM mathematical model to represent the flow around a body of revolution at an angle of attack. These involve the representation of the measured vorticity contours by a series of discrete Rankine vortices. The condition for the vortices to merge has been examined. Expressions for the Rankine vortex image within the circular body have also been developed. These techniques have application in the treatment of vortical flows close to circular bodies: submarines, airships, missiles, and offshore structures.

References

- ¹Lloyd, A. R. J. M., "Progress Towards a Rational Method of Predicting Submarine Manoeuvres," Paper 21, *Royal Inst. of Naval Architects Symposium on Naval Submarines*, Vol. II, Royal Inst. of Naval Architects, London, May 1983, p. 12.
- ²Lloyd, A. R. J. M., "Developments in the Prediction of Submarine Manoeuvres," *Undersea Defense Technology Conference Proceedings*, Microwave Exhibitions and Publishers, London, 1988, pp. 134-138.
- ³Mendenhall, M. R., Perkins, S. C., and Lesieur, D. J., "Prediction of the Aerodynamic Characteristics of Flight Vehicles in Large Unsteady Manoeuvres," *Proceedings of the 15th Congress of the International Council of the Aeronautical Sciences*, edited by P. Santini and R. Stautenbel, Vol. 2, AIAA, New York, 1986, pp. 662, 675.
- ⁴Glauert, H., *The Elements of Aerofoil and Airscrew Theory*, Cambridge Univ. Press, London, 1947.
- ⁵Lloyd, A. R. J. M., and Campbell I. M. C., "Experiments to Investigate the Vortices Shed from a Body of Revolution," *Aerodynamic and Related Hydrodynamic Studies Using Water Facilities*, AGARD CP 413, 59th Meeting of the AGARD Fluid Dynamics Panel Symposium, Monterey, CA, 1986, Paper 33, pp. 1-22.
- ⁶Lloyd, A. R. J. M., "Experiments to Investigate the Vorticity Shed by a Body of Revolution in Curved Flow," *Advances in Underwater Technology, Ocean Science and Offshore Engineering*, Vol. 15, Tech-

nology Common to Aero and Marine Engineering, Society for Underwater Technology, London, 1988, pp. 73-84.

⁷Freestone, M. M., "Vorticity Measurements by a Pressure Probe," *Aeronautical Journal*, Jan. 1988, p. 29-35.

Numerical Simulation of Vortex Unsteadiness on a Slender Body at High Incidence

David Degani*

NASA Ames Research Center, Moffett Field, California 94035

Introduction

RECENT studies (e.g., Refs. 1-3), conducted on two-dimensional and inclined cylinders of various cross-sectional shapes throughout the angle-of-attack range, have indicated that a high degree of flow unsteadiness may be present because of various phenomena. These include low-frequency three-dimensional effects, asymmetry-related vortex flipping, moderate-frequency von Kármán shedding, and higher frequency transition-related phenomena. In several cases, combinations of the phenomena have been found to coexist.

The study of Kourta et al.¹ presents information concerning small-scale, shear-layer vortices on two-dimensional cylinders for Reynolds numbers ranging from $Re_D = 2 \times 10^3$ to 6×10^4 . Hot-wire power spectra measured at points in the shear layer showed two peaks, the first corresponding to the von Kármán vortex shedding and the second to a much higher frequency associated with motion on the shear layer. Investigations of Wei and Smith² on two-dimensional circular cylinders provided additional evidence of the transition waves and showed that these waves are highly three dimensional.

Poll³ investigated the flow over a long cylinder (noncircular cross section) at Reynolds numbers ranging from 4.5×10^5 to 8.3×10^5 and angles of incidence ranging from 55 to 70 deg. He found that the boundary layer is susceptible to time-dependent disturbances that grow to large amplitude before the onset of transition. At the lower end of the Reynolds number range studied (prior to the transition to turbulence), a high-frequency rider was measured superimposed on a low-frequency von Kármán-like wave.

Preliminary computations⁴ of laminar flow around an ogive-cylinder body at large incidence indicated that the computed wake was asymmetric and also unsteady. Close examination of the solution showed that shear-layer vortices were being shed into the leeside vortex flowfield at a high frequency. Following the numerical finding, Degani and Zilliac⁵ conducted an experiment that demonstrated that the flowfield around an ogive-cylinder body at angles of attack above 30 deg was also highly unsteady. Three distinct unsteady flow phenomena were identified. These phenomena included a low-frequency von Kármán vortex shedding, a high-frequency shear-layer unsteadiness, and a vortex interaction at moderate frequency. The shear-layer fluctuations were found to decrease in amplitude and become intermittent as the angle of attack approach-

Received Oct. 15, 1990; revision received March 1, 1991; accepted for publication March 6, 1991. Copyright © 1991 by the American Institute of Aeronautics and Astronautics, Inc. No copyright is asserted under Title 17, U.S. Code. The U.S. Government has a royalty-free license to exercise all rights under the copyright claimed herein for Governmental purposes. All other rights are reserved by the copyright owner.

*Associate Professor, Faculty of Mechanical Engineering, on leave from Technion—Israel Institute of Technology, Haifa, Israel. Associate Fellow AIAA.